New Finite-Element Modelling of Subduction Processes in the Andes Using Realistic Geometries

Stefanie Zeumann, Rekha Sharma, René Gassmöller, Thomas Jahr, and Gerhard Jentzsch

Abstract

The aim of this work is the better understanding of geophysical processes in subduction zones by Finite element modelling. Here we study the effects of various parameters on the deformation and stress field. The tested parameters are the friction coefficient, convergence obliquity, bending of the subduction zone, realistic geometry and visco-elasticity. Increasing the friction coefficient from 0.0 to 0.4 increases the compression by 28 %. For both friction coefficients obliquity leads to higher compression compared to straight convergence. Comparison of the model results with real topographic data reveals considerable analogies even if crustal structure is generalised. To obtain a more realistic structure for the lithosphere we adopted the geometry from well constrained density models. For these models we chose the region in the South American subduction zone around Iquique in North Chile. Including viscosity in the models has a large effect on stress and strain. In a pure elastic model stress and strain develops nearly linear. In contrast curves for the visco-elastic models show a stress maximum and a zone of maximum curvature for the strain. The stress pattern agrees well with the earthquake distribution.

Keywords

Andes • Finite element • Geodynamic modelling • Subduction processes

1 Introduction

The strongest and most dangerous earthquakes on Earth often occur along subduction zones where oceanic lithosphere descends into the mantle. Although understanding the complex subduction processes has been a research object for many years there are still remaining problems and unknowns. The influence of subduction geometry on the stress and displacement fields in the upper crust is not well known. The coupling at the plate interface between oceanic and continental plates is so far not fully understood and parameters like friction coefficient or obliquity are still areas of research. Besides on site measurements and laboratory observations, numerical modelling is crucial for a better appreciation of the processes at convergent margins. In the last few years the South American subduction zone has been the topic of extensive research (e.g. Oncken et al. 2006; Barnes and Ehlers 2009; Köther et al. 2012).

Babeyko and Sobolev (2008) created 2D thermomechanical elasto-visco-plastic models of the Central Andes containing a subduction channel. They found a double compression zone in the upper part of the slab and a zone of extension below. The stress in the slab is mainly controlled by the overriding velocity and the direction of slab pull force. Hoffmann-Rothe et al. (2006) compared the friction coefficient for the northern and southern part of the Chilean subduction zone. Using critical taper theory they suggest

S. Zeumann (✉) • R. Sharma • T. Jahr • G. Jentzsch
Institute of Geosciences, Friedrich Schiller University, Burgweg 11, 07749 Jena, Germany
e-mail: stefanie.zeumann@uni-jena.de

R. Gassmöller
GFZ German Research Centre for Geosciences, Section Geodynamic Modelling, Telegrafenberg, 14473 Potsdam, Germany

C. Rizos and P. Willis (eds.), *Earth on the Edge: Science for a Sustainable Planet*, International Association of Geodesy Symposia 139, DOI 10.1007/978-3-642-37222-3_13,

Table 1 Parameters which are used for the elastic generalised models in Fig. 1

Parameter	Oceanic crust	Oceanic lithospheric mantle	Continental crust	Continental lithospheric mantle	Asthenosphere
Density (kg/m^3)	3,000	3,280	Upper 2,750	3,300	3,300
			Lower 2,950		
Young's modulus (GPa)	94.5	183	Upper 82.5	183	183
			Lower 94.5		

Poisson's ratio for all units is 0.25

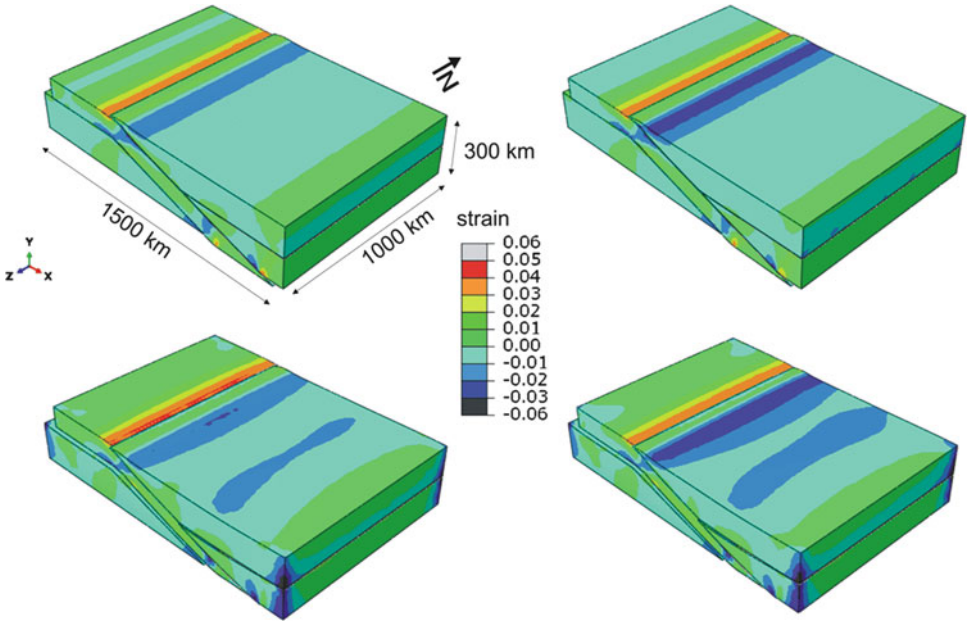

Fig. 1 East–west strain in models with straight (*top* row) or 20° oblique convergence (*bottom* row). The strain are shown after subduction of 1 million years with 6.5 cm/a, with friction coefficient of 0 (*left*) or 0.4 (*right*)

a reduced friction coefficient in the southern part which is probably compensated by an increasing width of the friction zone toward the south. In a 3D visco-elastic model Liu et al. (2002) simulate the spatial distribution of the Andean crustal shortening. The results show a nearly uniform short-term velocity gradient across the Andes, which is consistent with GPS data, and a concentrated long-term crustal shortening in the sub-Andean, which is consistent with geological observations.

In our study we investigate the effect of friction coefficient and oblique convergence on the deformation field at the surface using generalised models. Another major aspect in our paper is the geometry of the plate margin. The bending of the margin and the effect on the vertical deformation is investigated. Finally, we construct a 3D model with realistic geometry, using the Iquique segment of the South American subduction zone as an example, to test the influence of viscosity on the stress and deformation fields.

We develop dynamic 3D models based on the finite element method (FEM) using the commercial software package ABAQUS (Version 6.10, Online Tutorial 2010).

Even though temperature will influence the results it is so far not considered in the models. Creating a realistic 3D temperature model will be a future challenge.

2 Results and Discussion

2.1 Friction Coefficient and Convergence Obliquity

We construct finite element models with generalised geometries to study the effects of the friction coefficient and the convergence obliquity. The models have a constant slab dip angle of 18.4° (Hoffmann-Rothe et al. 2006) and a coupled zone between the plates in the depth range 10–50 km. Elastic parameters are taken from Babeyko and Sobolev (2008) and shown in Table 1.

After equilibrating the effect of gravity forces with pre-stresses a displacement corresponding to a velocity of 6.5 cm/a over a time of 1 million years is applied to the western edge and the bottom of the slab. In case of oblique

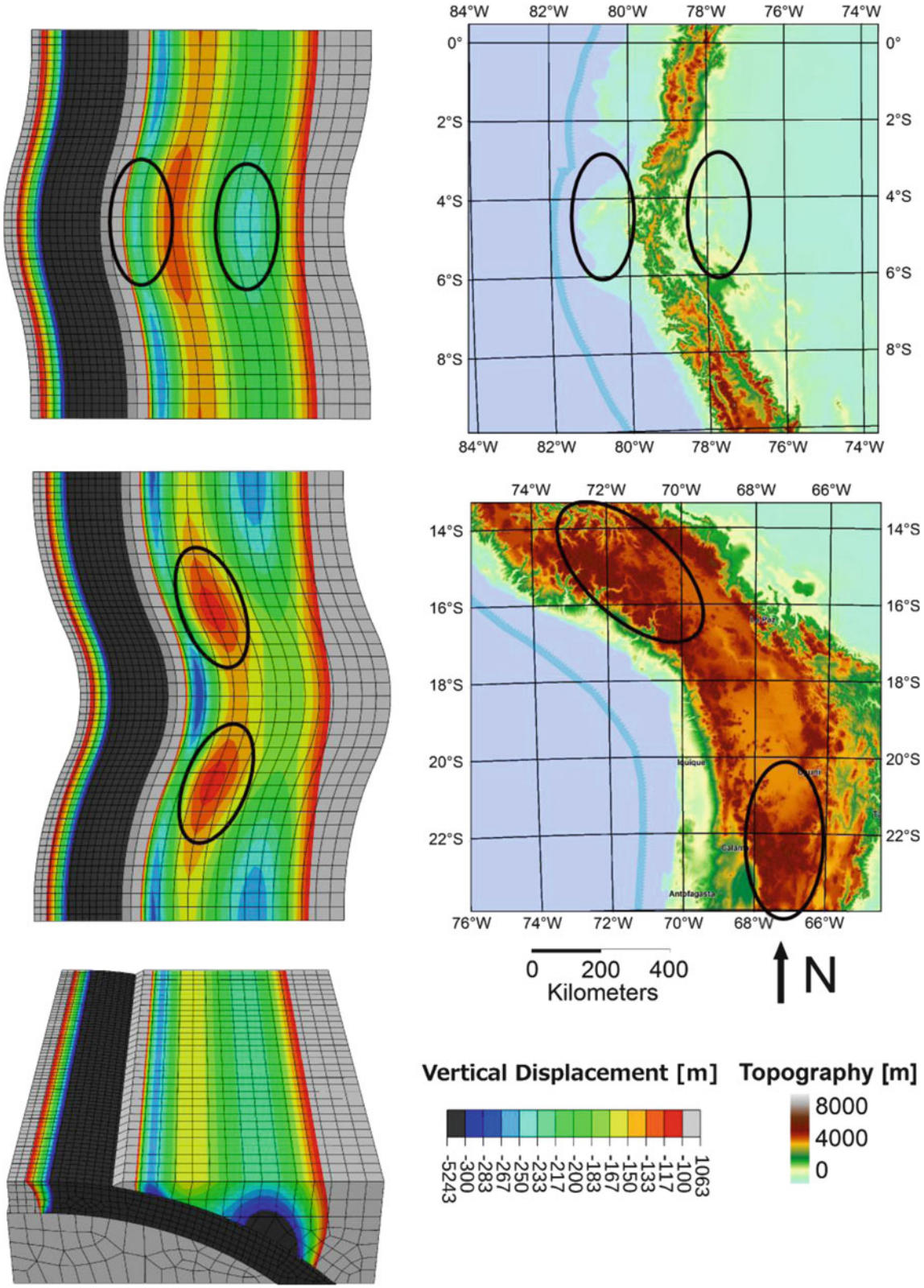

Fig. 2 Vertical displacement in models with seaward convex and concave subduction trench and comparison with the topography of equivalent regions in the Andes. The lower model is a reference model with a straight subduction trench. Regions of specific agreement are marked with *black ellipses* and the trench is shown in *light blue* after Oncken et al. (2006)

convergence the displacement was split in an east and a north component. The east and west edges of the models are not allowed to move in the east–west direction, north and south edges are fixed in north–south direction and bottom is fixed in north–south and vertical direction, except where displacements are applied. The models are 300 km deep and include crust, lithospheric mantle and the upper part of the asthenosphere. The continental crust is divided into upper and lower parts.

The horizontal strain normal to the trench reveals a region of compression in the fore arc (Fig. 1). Increasing the friction coefficient from 0.0 to 0.4 increases the compression by 26 % for straight convergence and by 28 % for oblique convergence. For both friction coefficients obliquity leads to higher compression, 2.4 % for coefficient 0.0 and 4.3 % for 0.4. For the oblique case a second compression zone in the back arc is visible.

2.2 Bent Subduction Zones

The geometries of many subduction zones show significant trench-parallel variations, which cannot be resolved by 2D models. Therefore, three different trench geometries (seaward convex bending, seaward concave bending, no bending) were taken from pre-existing data of the Andean subduction zone (Oncken et al. 2006) and transferred to an idealized geometry (Fig. 2). Although we apply a isostatic pressure field as initial condition, all models show slight subsidence due to the small deviations caused by no-slip boundary conditions and material interfaces. Hence, we do not interpret the absolute values but rather compare different areas of the model and their relative movement to an average value. The material properties of our model are summarized in Table 2. After 100,000 years of subduction with a convergence velocity of 8 cm/a a relative uplift for the volcanic arc and fore-arc of 30–60 m and a relative subsidence in the back-arc of 40 m develops in the case of the seaward convex model (Fig. 2 first row). In the seaward concave model there is an additional subsidence in the fore-arc (80 m) and additional uplift in the arc (on average 60 m). The most pronounced uplift of up to 100 m occurs not directly in front of the bend, but symmetrically at the sides. The back-arc also shows additional uplift of around 30 m in this case.

The comparison with measured topography from the GTOPO30 data set (USGS) reveals significant analogies, especially at the northern and southern borders of the Altiplano basin at 15°S and 22°S (Fig. 2, second row). Here as well as in the model the most uplift occurs at the sides instead of in front of the bend and the elevation is increased by around 1,000 m compared to the average height in the Altiplano basin.

Table 2 Material properties for models

Parameter	Oceanic crust	Continental crust	Lithospheric (cont. + oc.)	Asthenosphere
Density (kg/m^3)	3,000	2,950	3,300	3,300
Young's modulus (GPa)	99	99	185	185

All materials use a viscosity of 10^{23} Pa s

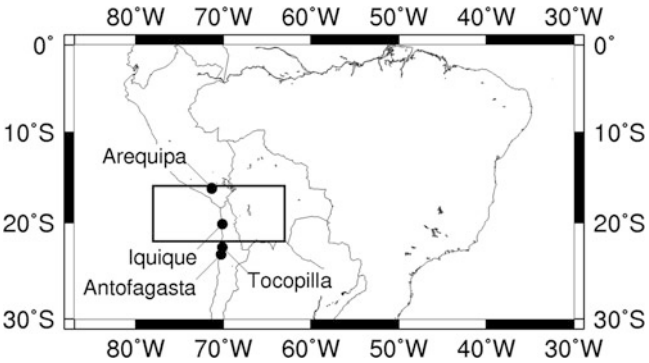

Fig. 3 Central part of South America. *Rectangle* marks the area of the model with realistic geometry

The comparison for the seaward convex model is more ambiguous. Although the relative uplift in the fore-arc and the relative subsidence in the back-arc match well, the arc uplift is not observed in recent topography. Instead, the volcanic arc around 5°S is several hundred meters lower than north and south of the bend. It is therefore possible that other features like the northern end of the flat-slab subduction interact with the geometrical features investigated in the model.

2.3 Realistic Geometries

The South American subduction zone along the Andes characterized by geo-hazards (e.g. Valdivia-earthquake 1960, Tocopilla 2007 or Maule earthquake 2010) is one of the most interesting regions to study dynamic processes related to subduction. To test the influence of including a realistic geometry as well as viscosity in the modelling, we developed a 3D model of the Iquique segment of the South American subduction zone between 16–22°S and 78–63°W (Fig. 3).

The geometries for the model were adopted from a well constrained density model by Tassara et al. (2006). The model includes the crust and the upper mantle down to a depth of 410 km and contains 16 different units with varying parameters as shown in the profile in Fig. 4.

It is well known that the Earth behaves mainly elastic for short time periods but over long timescales the Earth creeps by viscous flow (Ranalli 1995). Therefore the whole model behaves visco-elastic. The densities were taken from the

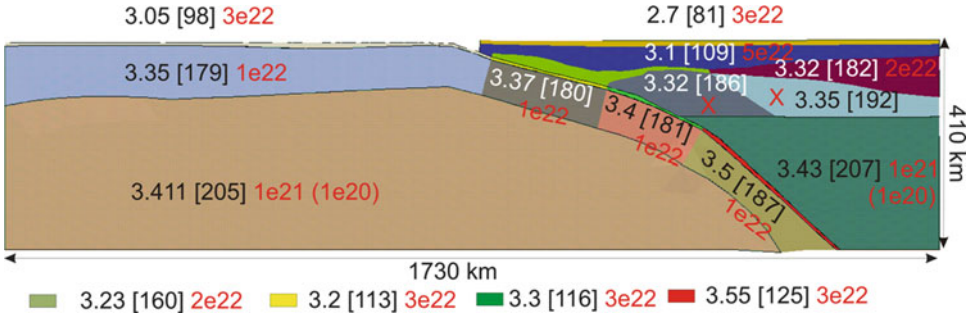

Fig. 4 Profile showing the material properties used in the 3D visco-elastic model, with realistic geometry adapted from the gravity model of Tassara et al. (2006). For each unit we state the density ($\times 10^3$ kg/m^3, from Tassara et al. 2006), Young's moduli in brackets (GPa, calculated from the seismic velocities of ANCORP 2003) viscosity in *red* (Pa s, from Liu et al. 2002) and viscosity in round brackets for reduced viscosity model. The cross denotes the *upper* asthenosphere with a viscosity of 10^{20} or 10^{19} Pa s for the reduced viscosity model

density model by Tassara et al. (2006). Young's moduli have been calculated using v_p velocities of the ANCORP profile (ANCORP Working group 2003) and the relationships

$$E = \rho v_s^2 (3v_p^2 - 4v_s^2)/(v_p^2 - v_s^2) \quad (1)$$

$$v_p = 3^{1/2} v_s. \quad (2)$$

The Poisson's ratio for every unit is 0.25. Viscosity depends on temperature, but over 100,000 years the temperature variation is only small, so temperature is not included in the model. Therefore different viscosities for the model units were chosen after Liu et al. (2002). After an equilibrium step for considering gravity, the Nazca plate moves with a convergence rate of 7.8 cm/a straight towards stable South America for 100,000 years (Somoza 1998). Velocities are applied at the western edge and the bottom of the slab. North and south edge are fixed in north–south direction, bottom fixed in vertical direction and east and west edges are fixed in east–west direction except where velocities are applied. The oblique movement of the Nazca plate towards South America will be included in future models because obliquity has an influence on the results (Fig. 1).

The depth limit for frictional coupling can be estimated from the depth of the seismogenic zone (Wang and Suyehiro 1999) or from modelling of geodetic data. Tichelaar and Ruff (1991) concluded that coupling in the northern Chile region extends at least as deep as 45–48 km, based on the depth of large underthrusting earthquakes. Hoffmann-Rothe et al. (2006) estimated a lower coupling depth of 33 km from inversion of GPS surface velocities. Here we choose to use 40 km as friction depth, and a friction coefficient of 0.1.

The horizontal strain component normal to the trench at the surface after 100,000 years shows compression in the fore-arc and a zone of extension 300–600 km away from the trench which correspond to the Altiplano plateau (Fig. 5). The strain is plotted for a visco-elastic model with mantle viscosities as shown in Fig. 4.

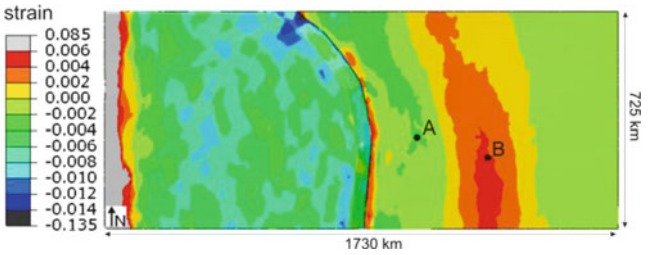

Fig. 5 East–west strain after 100,000 years. Point A in *fore-arc* is used for comparison with the results of Klotz et al. (2006) and point B in the *back-arc* marks a reference point also discussed in Fig. 7

Klotz et al. (2006) determined strain rates derived from GPS data in the fore-arc. For the Antofagasta region, which is situated 2° south of the model area they found -0.124 ± 0.042 μstrain/a in east–west and -0.05 ± 0.039 μstrain/a in north–south direction, which means shortening. But this region was affected by the Antofagasta-earthquake in 1995. For the area north of the Antofagasta region their results show compression as well as extension in the fore-arc with magnitudes lower than 0.1 μstrain/a. To compare our results we assume a linear development for the calculated strain over the last modelled 10,000 years. For point A in Fig. 5 this leads to a strain rate of -0.015 μstrain/a in east–west direction, which is one order of magnitude lower compared to Klotz et al. (2006).

The stress distribution on the surface of the subducting slab after 100,000 years is shown in Fig. 6. The stress pattern agrees well with the earthquake distribution in the region. The results show a stress accumulation in zone A which can be compared to a region with higher seismicity. The high stress belt (B) marks the beginning of the continental asthenosphere, where material parameters change (Fig. 4). It is 300 km away from the trench and 150 km deep.

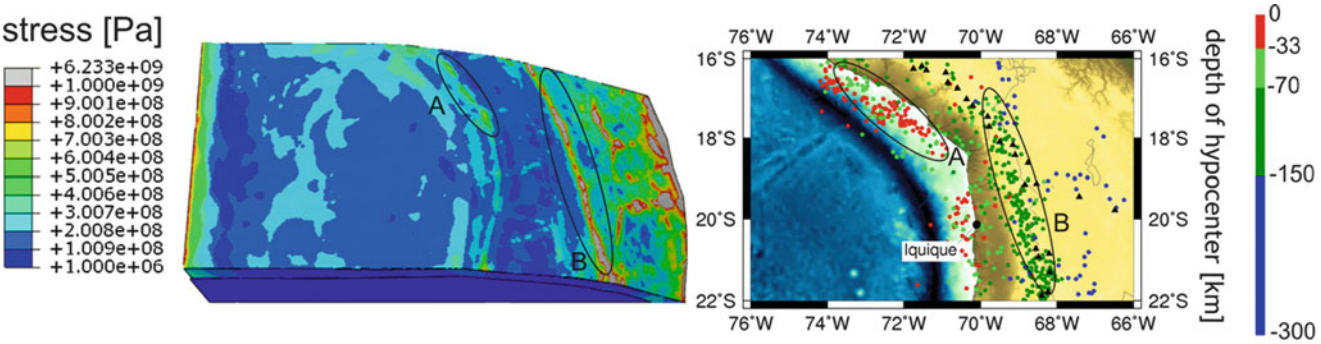

Fig. 6 *Left*: Distribution of von Mises stress in the 3D model of the Iquique segment. The stresses are taken at slab surface after 100,000 years. *Right*: Earthquake distribution (USGS) in the model area during the last 40 years. Only events with magnitude > 5 are shown. *Colour* represents depth of hypocenters. *Black triangle* denotes volcanoes

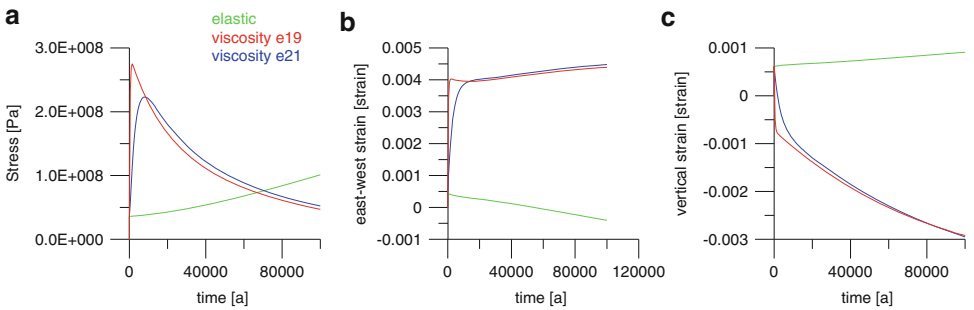

Fig. 7 Comparison of the results for models with visco-elastic versus elastic rheology. Stress (**a**), east–west strain (**b**) and vertical strain (**c**) are shown for point B in Fig. 5. *Green* curves represent the elastic model, *blue* curves the visco-elastic model with parameters as shown in Fig 4, and *red* curves represent a visco-elastic model with reduced mantle viscosity

This fits nearly the line of green marked earthquakes below the volcanic arc.

To show the effect of viscosity the results for different model rheologies are compared (Fig. 7). The results are shown for point B in the back-arc of the model marked in Fig. 5. The green curves are the results for a purely elastic model, where no viscosity is included. Blue curves represent the results for the visco-elastic model with the parameter shown in Fig. 4. Red curves show the results for a similar model but with reduced mantle viscosity of 10^{19} Pa s for the upper continental asthenosphere (red crosses in Fig. 4) and 10^{20} Pa s for the asthenosphere.

For the elastic case the stress and strain increases nearly linear over the total time. Stress for the models including viscosity increases linear at the beginning until it reaches a maximum, then drops (Fig. 7). At the same time as the stress maximum a zone of maximal curvature occurs in the horizontal and vertical strain (Fig 7). This denotes the point where viscosity starts to work and magnitude and time is controlled by the viscosity. Reduced viscosity leads to an earlier and higher maximum in stress but do not change the characteristic of the curves. Comparing elastic and visco-elastic models the slope for the strain curves shows an opposite sign. In conclusion, including viscosity in the modelling has a large effect on stress and strain.

3 Conclusions

Our geodynamic modelling shows that different model assumptions about rheology and geometry have a large influence on the development of displacements and stress in a subduction zone. We find that several of the topographic features of the Andes could be caused by the bent trench without considering additional contributions like crustal structure, plate velocities, sedimentation rate, convergence direction or history. Of course this does not exclude these effects for topography or crustal deformation. The result of generalised models show that friction coefficient and convergence obliquity influence the strain field. Oblique convergence and increasing the friction coefficient leads to higher compression. In the model with more realistic geometries the stress pattern on the subducting slab agrees well with the earthquake distribution in the investigation area. Including viscosity in the model has a large effect on stress and strain. In a pure elastic model stress and strain

develops nearly linear. In contrast curves for the visco-elastic models show a stress maximum and a zone of maximum curvature for the strain. Magnitude and time of these features depend on viscosity. A reduced mantle viscosity leads to an earlier and higher stress maximum.

Acknowledgements This work is part of the project IMOSAGA, a cooperation with University Kiel and TU Munich within the German priority program "Mass transport and mass distribution in the system Earth" (SPP 1257). The research is supported by the German research foundation (DFG). We thank the reviewers for improving the paper by their helpful comments and recommendations.

References

ABAQUS (2010) Version 6.10. Dassault Systèmes Simulia Corp., Providence. Link to online tutorial: http://abaqus.civil.uwa.edu.au:2080/v6.10/index.html

ANCORP Working group (2003) Seismic imaging of convergent continental margin and plateau in the central Andes (Andean Continental Research Project 1996 (ANCORP'96)). J Geophys Res 108(B7):2328. doi:10.1029/2002JB001771

Babeyko AY, Sobolev SV (2008) High-resolution numerical modelling of stress distribution in visco-elasto-plastic subducting slabs. Lithos 103:205–216. doi:10.1016/j.lithos.2007.09015

Barnes JB, Ehlers TA (2009) End member models for Andean Plateau uplift. Earth Sci Rev 97:105–132. doi:10.1016/j.earscirev.2009.08.003

Hoffmann-Rothe A, Kukowski N, Dresen G, Echtler H, Oncken O, Klotz J, Scheuber E, Kellner A (2006) Oblique convergence along the Chilean margin: partitioning, margin-parallel faulting and force interaction at the plate interface. In: Oncken O, Chong G, Franz G, Giese P, Götze H-J,Ramos VA, Strecker MR, Wigger P (eds) The Andes—active subduction orogeny, vol 1, Frontiers in earth science series. Springer, Heidelberg, pp 125–146

Klotz J, Abolghasem A, Khazaradze G, Heinze B, Vietor T, Hackney R, Bataille K, Maturana R, Viramonte J, Perdomo R (2006) Long-term signals in the present-day deformation field of the Central and Southern Andes and constraints on the viscosity of the earth's upper mantle. In: Oncken O, Chong G, Franz G, Giese P, Götze H-J, Ramos VA, Strecker MR, Wigger P (eds) The Andes—active subduction orogeny, vol 1, Frontiers in earth science series. Springer, Heidelberg, pp 65–89

Köther N, Götze H-J, Gutknecht BD, Jahr T, Jentzsch G, Lücke OH, Mahatsente R, Sharma R, Zeumann S (2012) The seismically active Andean and Central American margins: can satellite gravity map lithospheric structures? J Geodyn 59-60C. doi:10.1016/j.jog.2011.11.004

Liu M, Yang Y, Stein S, Klosko E (2002) Crustal shortening and extension in the Central Andes: insights from a viscoelastic model. In: Stein S, Freymueller JT (eds) Plate boundary zones, vol 30, Geodyn Ser. AGU, Washington, DC, pp 325–339. doi:10.1029/GD030p0325

Oncken O, Chong G, Franz G, Giese P, Götze H-J, Ramos VA, Strecker MR, Wigger P (eds) (2006) The Andes—active subduction orogeny. Frontiers in earth science series, vol 1. Springer, Heidelberg, pp 3–27

Ranalli G (1995) Rheology of the earth, 2nd edn. Chapman & Hall, London, p 413

Somoza R (1998) Updated Nazca (Farallon)-South America relative motions during the last 40 my: implications for mountain building in the central Andean region. J South Am Earth Sci 11(3):211–215. doi:10.1016/S0895-9811(98)00012-1

Tassara A, Götze H-J, Schmidt S, Hackney R (2006) Three-dimensional density model of the Nazca plate and the Andean continental margin. J Geophys Res 111:B09404. doi:10.1029/2005JB003976

Tichelaar BW, Ruff LJ (1991) Seismic coupling along the Chilean subduction zone. J Geophys Res 96(B7):11997–12022. doi:10.1029/91JB00200

Wang K, Suyehiro K (1999) How does plate coupling affect crustal stresses in northeast and southwest Japan? Geophys Res Lett 26(15):2307–2310. doi:10.1029/1999GL900528